THE ASTROPHYSICAL JOURNAL, 331:L41–L45, 1988 August 1

HIGH-RESOLUTION VLA OBSERVATIONS OF THE W3(OH) METHANOL MASERS

K. M. MENTEN,[1,2] K. J. JOHNSTON,[3,4] E. J. WADIAK,[5] C. M. WALMSLEY,[1] AND T. L. WILSON[1,3]
Received 1988 March 16; accepted 1988 May 4

ABSTRACT

VLA observations of the $9_2 \rightarrow 10_1$ A^+ transition of methanol (CH_3OH) with 0\".08 resolution toward W3(OH) are presented. The emission arises from at least eight regions situated on a crescent-shaped arc which is aligned in approximately the north-south direction in front of the compact H II region. The angular sizes of the individual regions are less than 0\".04, the brightness temperature of the most intense region is at least 10^7 K. A VLBI experiment gave no fringes, implying a lower limit of 0\".003 to the angular size or an upper limit of 2×10^9 K to the brightness temperature of the strongest feature. There is a close resemblance between the spatial distribution of the CH_3OH and OH maser emission. We conclude that the conditions required for maser action of both species must be closely related.

Subject headings: interstellar: molecules — masers — nebulae: H II regions — stars: formation

I. INTRODUCTION

Millimeter-wave and centimeter-wave lines of interstellar methanol (CH_3OH) have been observed toward the ultracompact H II region W3(OH) in absorption as well as in emission (see Menten *et al.* 1986*a*, *b*). Most spectacular appear the transitions at 23.1, 19.9, and 12.2 GHz, which are masing and have flux densities of 10, 50, and 700 Jy, respectively (Wilson *et al.* 1984, 1985; Batrla *et al.* 1987). Of these transitions, only the 23.1 GHz $9_2 \rightarrow 10_1 A^+$ line lies within a frequency band of the Very Large Array of the NRAO.[6] The 2\" resolution observations by Menten *et al.* (1985) have confirmed the maser nature of this emission and its positional coincidence with the compact continuum source. Moreover, these measurements showed a general trend for the methanol emission to be concentrated toward the western part of the continuum source, where a band of OH maser spots extends in the N–S direction (Reid *et al.* 1980; Norris, Booth, and Diamond 1982) and NH_3 and OH absorption, as well as quasi-thermal OH emission is found (Guilloteau, Stier, and Downes 1983; Guilloteau, Baudry, and Walmsley 1985; Reid, Myers, and Bieging 1987). However, the vast difference in spatial resolution between these CH_3OH observations and the VLBI and MERLIN measurements of OH (2\" vs. ~ 0\".01) does not allow detailed comparison of the emission regions of the two molecules.

To learn more about the spatial distribution of the CH_3OH masers, in particular their relationship to the OH masers and the compact continuum, we have reobserved the $9_2 \rightarrow 10_1$ A^+ line using the VLA in the A configuration. To obtain even higher angular resolution, we also conducted a VLBI experiment.

II. OBSERVATIONS

The VLA experiment was carried out on 1986 May 19 using 23 antennas in the A configuration. The total bandwidth was 0.78 MHz and 64 spectral channels gave a velocity resolution of 0.16 km s^{-1}. The band was centered at an LSR velocity of 44.2 km s^{-1} assuming a rest frequency of 23121.024 MHz (Mehrotra, Dreizler, and Mäder 1985). 3C 84, which was assumed to have a flux density of 42 Jy, was used for phase and amplitude calibration. The data were analyzed using the AIPS processing system. The strongest spectral component at −43.2 km s^{-1} was used in the self-calibration scheme described by Schwab (1980). Maps were made with a cell size of 0\".02 using natural weighting. This resulted in a synthesized beam of 0\".085 × 0\".082, with P.A. 27°. Spectral features were regarded as real if their intensity was at least 4 times the rms noise (typically 0.05 Jy per beam) in the channel maps and only if they appeared in at least two adjacent channels. The relative positions of individual emission features were determined from the maps by applying a two-dimensional Gaussian fit. To estimate radial velocities and line widths, Gaussians were fitted to the line profiles. Table 1 lists the parameters of the features that we have fitted. Some other weaker or confused features are certainly present. A continuum map was constructed by averaging channels with no line emission. To improve the signal-to-noise ratio, a 1000 $k\lambda$ taper was applied to these continuum data, resulting in a synthesized beam of 0\".20 × 0\".16 and P.A. 81°.

A four-station Mk II VLBI experiment between Haystack Observatory, Maryland Point, Effelsberg, and Green Bank was performed on 1987 February 19. Due to poor receiver performance at Maryland Point and a snowstorm at Effelsberg, the most sensitive data were taken between Haystack and Green Bank. The minimum fringe spacing was 0\".003. We recorded a bandwidth of 2 MHz and used 96 spectral channels. 3C 84 displayed a fringe amplitude of 0.20 on the Green Bank–Haystack baseline. The CH_3OH spectrum clearly appeared in the autocorrelation spectrum at the Green Bank and Haystack sites with a peak amplitude of 0.012 at both stations. Assuming a maximum interferometer flux density of 42 Jy for 3C 84, a cross correlation of 0.005 was expected for the 9 Jy spectral feature in W3(OH), if it were unresolved. An upper limit to the correlated signal of 0.001 puts a lower limit of 0\".003 to its size or an upper limit of 2×10^9 K to its brightness temperature, assuming a single circular Gaussian source.

III. RESULTS AND DISCUSSION

Maps of the emission in the individual velocity channels which were obtained after subtracting the continuum emission

[1] Max-Planck-Institut für Radioastronomie.
[2] Harvard-Smithsonian Center for Astrophysics.
[3] E. O. Hulburt Center for Space Research, Naval Research Laboratory.
[4] Senior Humboldt Awardee at the Max-Planck-Institut für Radioastronomie.
[5] National Radio Astronomy Observatory.
[6] The National Radio Astronomy Observatory is operated by Associated Universities, Inc., under contract with the National Science Foundation.

TABLE 1

OBSERVATIONAL RESULTS

Clump Number	$\Delta\alpha$[a]	$\Delta\delta$[a]	v_{LSR}[b] (km s^{-1})	Δv[b] (km s^{-1})	S[c] (Jy per beam)	T_B[d] (10^6 K)	τ[e]
I	−0″26	0″87	−43.15	0.35	0.3	0.4	−6.9
	−0.26	0.75	−42.51	0.29	1.2	1	−6.9
II	−0.46	0.53	−43.93*	0.3*	0.3	0.4	−5.2
	−0.47	0.47	−44.40*	0.3*	0.4	0.4	−5.2
III	−0.52	0.14	−44.12	0.40	0.7	0.9	−6.2
	−0.49	0.01	−43.93	0.35	0.3	0.4	−5.4
IV	−0.40	−0.34	−43.15	0.38	9.4	12	−8.6
	−0.37	−0.49	−43.64	0.38	0.4	0.5	−5.8

[a] Position offsets are relative to $\alpha(1950) = 02^h23^m16^s.5$, $\delta(1950) = 61°38'57''.0$. *Relative* positions were determined by fitting Gaussian brightness distributions to the single-channel maps and are accurate to better 0″01. The *absolute* positional accuracy is estimated to be 0″1.

[b] LSR velocities and line widths were determined from Gaussian fits. For some components, such fits were not possible. For these, estimated v_{LSR} and Δv values are given and denoted by asterisks.

[c] Peak flux density.

[d] Lower limits on the brightness temperature, assuming that the maser spots have sizes ≤ 0″04, i.e., are unresolved in our 0″08 synthesized beam.

[e] Upper limits on optical depths were determined from a comparison of our maser positions with the 23.7 GHz continuum map of Guilloteau *et al.* 1983 assuming exponential amplification of the background continuum.

are shown in Figure 1. In Figure 2, maps of the velocity-integrated line emission and the continuum are presented. The signal-to-noise ratio in our smoothed continuum map is significantly lower than that of the map measured by Guilloteau, Stier, and Downes (1983) which had a comparable resolution, but the maps are in general agreement. From Figures 1 and 2, the CH_3OH emission region consists of at least eight spots aligned in a crescent shape in the N–S direction. A Gaussian fit analysis shows that the individual spots are not resolved in our 0″08 beam, implying lower limits for the true brightness temperatures between a few times 10^5 and 10^7 K. These large brightness temperatures make it clear that we are observing maser emission. The velocities of the maser spots range between −44.4 and −42.5 km s^{-1} (see Table 1). No velocity gradient in the N–S direction is apparent. We find that the maser components cluster together in several groups of at least two members each. The eight components listed in Table 1 appear to form four close pairs, denoted as I to IV. These have separations between 0″07 and 0″15, corresponding to 2–5×10^{15} cm at a 2.2 kpc distance for W3(OH). Neighboring pairs are separated by typically 0″42 (1.3×10^{16} cm). The velocity differences of the members of a pair are between 0.2 and 0.6 km s^{-1}. There is evidence in our data for weak features below our 4 σ acceptance limit.

Since other methanol transitions show absorption toward W3(OH) covering the same velocity range as the maser emission (Menten *et al.* 1985, 1986*a*, *b*), it is straightforward to assume that the methanol masers are in front of the compact H II region and amplify the background continuum. By comparing the positions and brightness temperatures of the maser spots with the 23 GHz continuum map, we derive the upper limits for the maser optical depths listed in Table 1.

Interferometric observations have shown that the dense molecular material probed by quasi-thermal OH emission and absorption (Guilloteau, Baudry, and Walmsley 1985), NH_3 absorption (Guilloteau, Stier, and Downes 1983; Reid, Myers, and Bieging 1987), and OH masers (Moran *et al.* 1978; Reid *et al.* 1980; Norris, Booth, and Diamond 1982; Baudry *et al.* 1988) covers the western part of the compact continuum source. In Figure 3, we show a comparison of the CH_3OH maser positions with the distribution of the OH maser emission measured in different transitions. Obviously, the methanol masers delineate the eastern edge of the area that contains the bulk of the OH maser centers. Whereas we find OH maser spots in the vicinity of all the methanol maser components, no methanol emission is detected toward the westernmost OH maser centers. A detailed comparison of OH and CH_3OH velocities is not straightforward, because (1) absolute OH positions from VLBI observations have typical errors of 0″1–0″2 and (2) OH velocities (except for the 4765 MHz transition) are affected by the Zeeman effect. A VLBI experiment by Baudry *et al.* (1988) has shown that emission from the 4765 MHz line emerges from the three regions denoted A, B, and C in Figure 3. For the 6035 MHz OH line, Moran *et al.* (1978) have been able to identify left-hand and right-hand circularly polarized features as Zeeman pairs, allowing the determination of magnetic fields and the "true" velocities of these maser components. The methanol clumps II and IV have nearby 4765 and 6035 MHz OH counterparts. For clump II, the mean CH_3OH velocity is −44.2 km s^{-1}, while the OH velocity centroids are −43.2 and −45.2 km s^{-1} for the 4765 and 6035 MHz lines, respectively. In clump IV, CH_3OH velocities between −43.6 and −43.2 km s^{-1} compare with OH values of −43.5 km s^{-1} (4765 MHz) and −43.2 km s^{-1} (6035 MHz). The 6035 MHz OH cluster near clump I has a large velocity dispersion with velocities (between −48.1 and −43.5 km s^{-1}), somewhat different from the methanol velocities (−43.2 and −42.5 km s^{-1}). In conclusion, the methanol velocities are, in general, within the range of the values found for neighboring OH masers.

The fact that the methanol masers are not affected by Zeeman splitting makes it easier to analyze the kinematics of maser groups. It is very striking that methanol, like OH (see Reid *et al.* 1980), seems to cluster on a size scale of $\sim 3 \times 10^{15}$ cm^{-2}. As noted above, some of the clusters appear to be identical with the groupings identified in OH. Applying the virial theorem and taking a typical velocity dispersion of 0.5 km s^{-1} for such a cluster, we derive a mass of order 0.03 $M_\odot$ and a

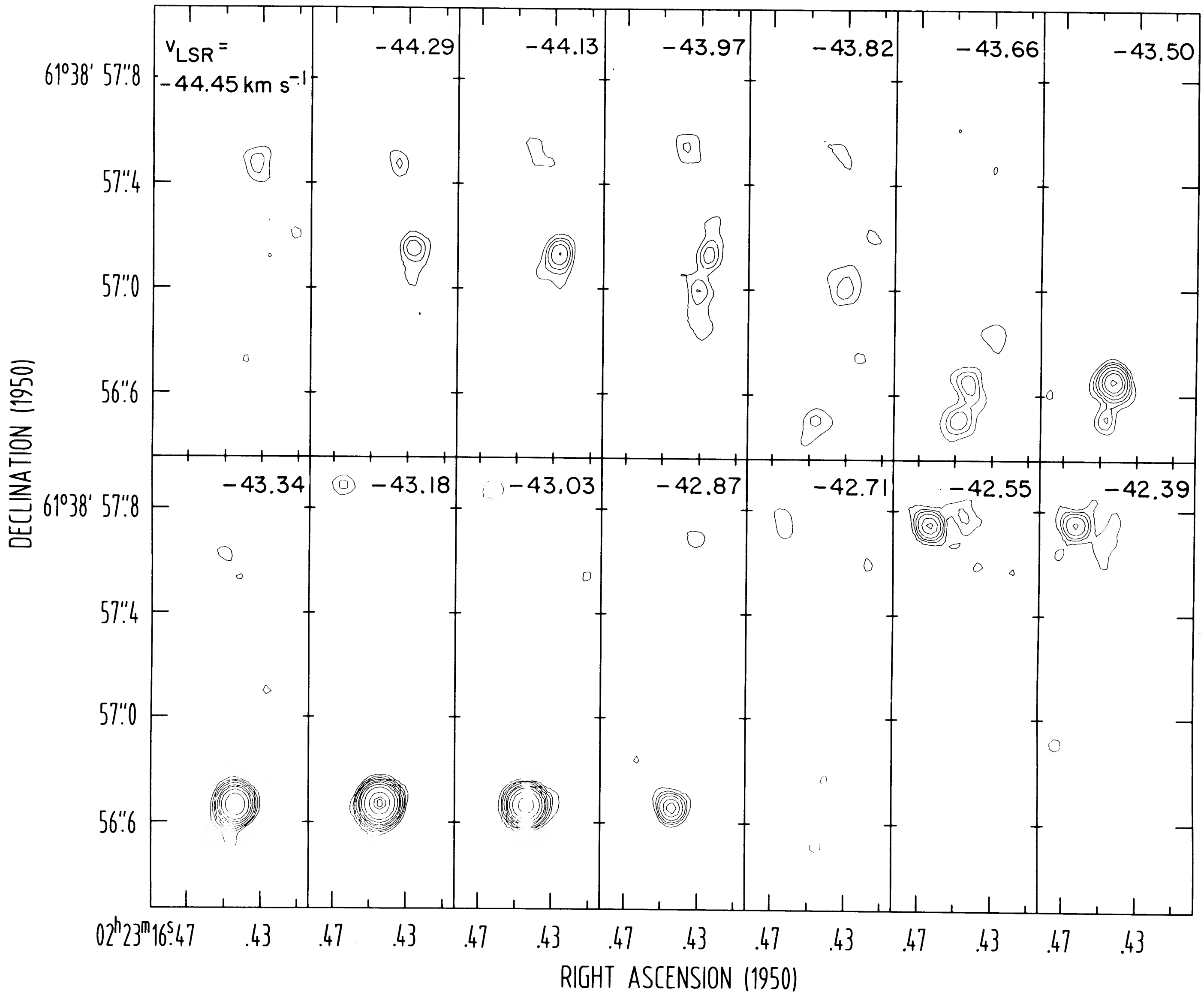

FIG. 1.—Maps of individual spectral channels for velocities between -44.45 km s^{-1} and -42.39 km s^{-1}. Continuum emission has been subtracted. Contour levels are 3, 5, 7, 10, 15, 20, 30, 50, 100, 150, 170 times 50 mJy beam^{-1} which is the average 1 σ noise in the maps. The size of the synthesized beam is 0″.085 × 0″.082.

density of order 10^9 cm^{-3}. This density is higher than values suggested for OH masers.

Our results show that the strongest $9_2 \rightarrow 10_1\ A^+$ maser at $v = -43.2$ km s^{-1} has a brightness temperature of at least 10^7 K. If, as we suspect, the pump mechanism involves radiative excitation to the first torsionally excited state ($v_t = 1$) with a pump rate $\Gamma \approx 1$ s^{-1} (Menten *et al.* 1986*b*), we can estimate the mean intensity required to saturate the maser as $T_{\rm sat} \approx \Gamma(h\nu/k)/A$, where ν is the line frequency, and A is the Einstein A-value ($\sim 2 \times 10^{-8}$ s^{-1}) (e.g., Reid and Moran 1981) and obtain $T_{\rm sat} \approx 5 \times 10^7$ K. Our rough limits on the brightness temperatures together with the uncertainty about the beaming of the masers prohibit a conclusive statement about the degree of saturation. There is no indication of extreme line narrowing or of variability which an unsaturated maser might be expected to show.

The most interesting feature of our results is the arc-shaped nature of the CH_3OH maser distribution (e.g., Fig. 2). This suggests that the methanol is mainly present along the inner edge of the cloud responsible for OH masers and NH_3 absorption. Reid *et al.* (1980) have pointed out that in a cloud collapsing with an $r^{-0.5}$ velocity distribution, one expects to see the maximum coherence length on a cone of opening angle 35° and axis along the line of sight. If the methanol is present in a shell, one would then expect to observe a ring of masers of constant velocity. Our observations place the center of such a ring on the eastern edge of the compact H II region. It would be surprising to find the exciting star of the H II region so far offset from the centroid of the continuum emission, but this cannot be excluded. Guilloteau, Stier, and Downes (1983) have pointed out that another interpretation of the OH and NH_3 data is that the OH masers are to be found in an inclined disk of molecular material. In this case, only the foreground portion is seen in OH and CH_3OH masers if they amplify the continuum background.

We thank Dr. P. J. Diamond for assistance with the reduction of the VLBI data.

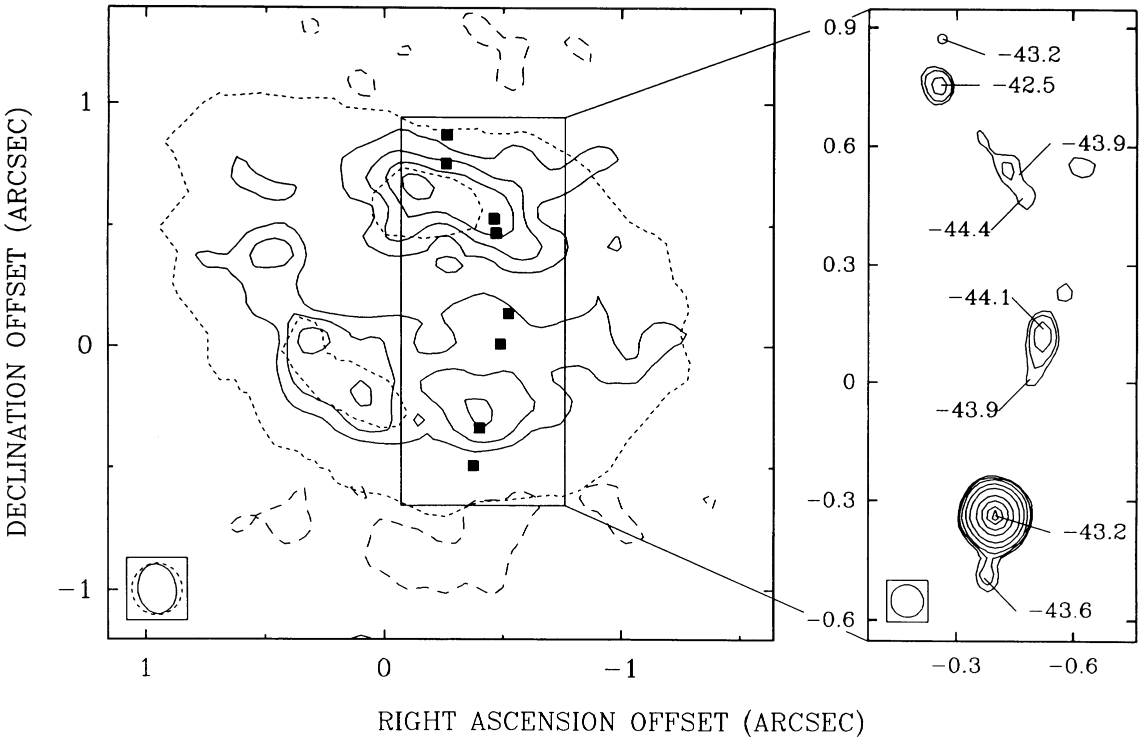

FIG. 2.—The left-hand panel shows our smoothed continuum map obtained by averaging the channels with no line emission. The solid lines represent 30%, 50%, 70%, and 90% of the peak flux density of 112 mJy beam^{-1}. This corresponds to a brightness temperature of 7750 K. The big dashes show the −30% contour level. The lowest contour value corresponds to 3 times the rms noise in the map. For comparison, the 10% and 70% contours of the 23.7 GHz continuum map of Guilloteau *et al.* (1983) are shown as dotted lines. The restoring beams of our (*solid*) and Guilloteau *et al.*'s (*dotted*) map are shown to the lower left. The filled squares denote the positions of the $9_2 \rightarrow 10_1\ A^+$ maser spots. The rectangle delimits the extent of the map of the velocity-integrated flux density observed in the $9_2 \rightarrow 10_1\ A^+$ line which is shown in the right-hand panel. Contours are 0.16, 0.20, 0.28, 0.48, 0.80, 1.6, 2.4, 3.2, and 3.6 Jy beam^{-1} km s^{-1}. The peak flux density and the 1 σ noise in the map are 3.81 and 0.04 Jy beam^{-1} km s^{-1}, respectively. Positions and velocities (in km s^{-1}) of the individual maser features are indicated. The weak northernmost feature, although clearly discernible in the single channel maps (Fig. 1), does not show up prominently in the integrated intensity map because of its lower signal-to-noise ratio. The beam shape is shown in the bottom left corner. The (0, 0) position in both panels corresponds to $\alpha(1950) = 02^h23^m16\overset{s}{.}5$, $\delta(1950) = 61°38'57\overset{''}{.}0$.

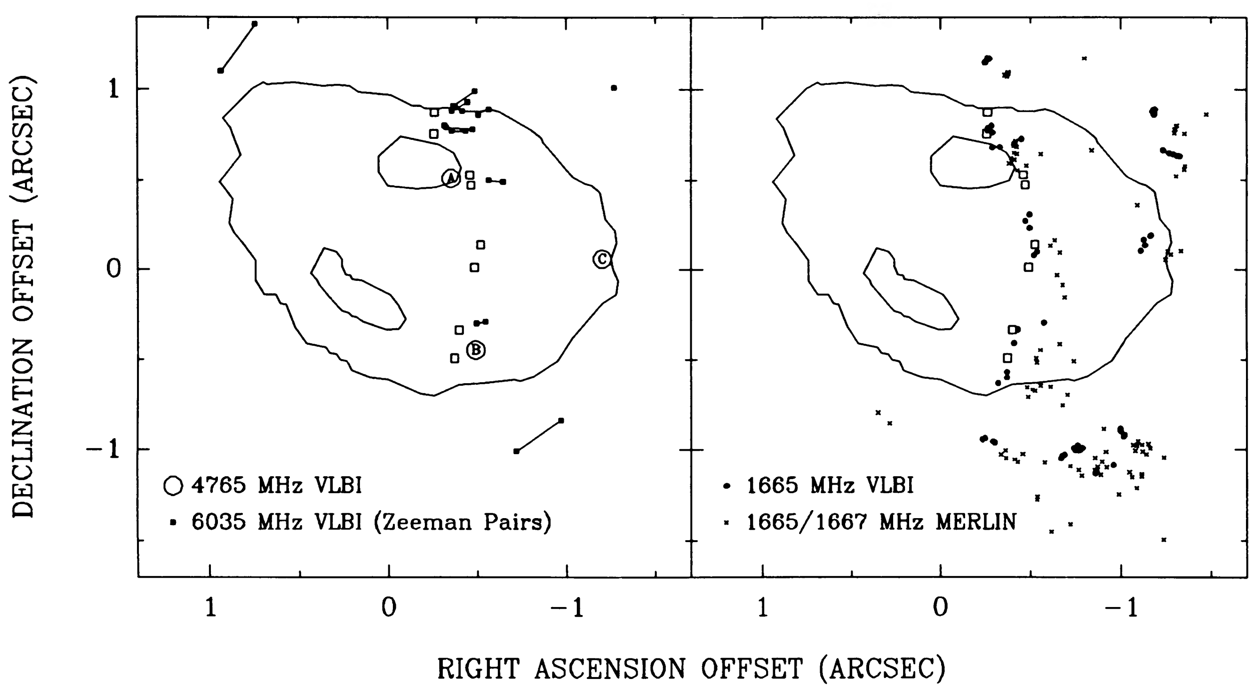

FIG. 3.—Comparison of the positions of the $9_2 \rightarrow 10_1\ A^+$ methanol masers (*open squares*) with OH masers. The left-hand panel shows (*small filled squares joined by lines*) 6035 MHz Zeeman pairs identified by Moran *et al.* (1978) together with the three 4765 MHz complexes (A, B, and C) reported by Baudry *et al.* (1988). In the right-hand panel crosses show the positions of the 1665/1667 MHz OH masers as determined by Norris *et al.* (1982) using the MERLIN interferometer. Dots show the VLBI positions of the 1665 MHz masers (Reid *et al.* 1980). The background contours in both panels are the 10% and 70% contours of the continuum map of Guilloteau *et al.* (1983). The (0, 0) position is the same as in Fig. 2.

REFERENCES

Batrla, W., Matthews, H. E., Menten, K. M., and Walmsley, C. M. 1987, *Nature*, **326**, 49.
Baudry, A., Diamond, P. J., Graham, D., Walmsley, C. M., and Booth, R. S. 1988, *Astr. Ap.*, in press.
Guilloteau, S., Baudry, A., and Walmsley, C. M. 1985, *Astr. Ap.*, **153**, 179.
Guilloteau, S., Stier, M. T., and Downes, D. 1983, *Astr. Ap.*, **126**, 10.
Mehrotra, S. C., Dreizler, H., and Mäder, H. 1985, *Zs. Naturforsch.*, **40a**, 683.
Menten, K. M., Johnston, K. J., Wilson, T. L., Walmsley, C. M., Mauersberger, R., and Henkel, C. 1985, *Ap. J.* (*Letters*), **293**, L83.
Menten, K. M., Walmsley, C. M., Henkel, C., and Wilson, T. L. 1986*a*, *Astr. Ap.*, **157**, 318.
Menten, K. M., Walmsley, C. M., Henkel, C., Wilson, T. L., Snyder, L. E., Hollis, J. M., and Lovas, F. J. 1986*b*, *Astr. Ap.*, **169**, 271.
Moran, J. M., Reid, M. J., Lada, C. J., Yen, J. L., Johnston, K. J., and Spencer, J. H. 1978, *Ap. J.* (*Letters*), **224**, L67.
Norris, R. P., Booth, R. S., and Diamond, P. J. 1982, *M.N.R.A.S.*, **201**, 209.
Reid, M. J., Haschick, A., Burke, B. F., Moran, J. M., Johnston, K. J., and Swenson, G. W., Jr. 1980, *Ap. J.*, **239**, 89.
Reid, M. J., and Moran, J. M. 1981, *Ann. Rev. Astr. Ap.*, **19**, 231.
Reid, M. J., Myers, P. C., and Bieging, J. H. 1987, *Ap. J.*, **312**, 830.
Schwab, F. 1980, *Proc. Soc. Photo.-Opt. Instr. Eng.*, **231**, 18.
Wilson, T. L., Walmsley, C. M., Menten, K. M., and Hermsen, W. 1985, *Astr. Ap.*, **147**, L19.
Wilson, T. L., Walmsley, C. M., Snyder, L. E., and Jewell, P. R. 1984, *Astr. Ap.*, **134**, L7.

K. J. JOHNSTON: E. O. Hulbert Center for Space Research, Naval Research Laboratory, Code 4130, Washington, DC 20375

K. M. MENTEN: Harvard-Smithsonian Center for Astrophysics, 60 Garden Street, Cambridge, MA 02138

E. J. WADIAK: Interferometrics, Inc., 8150 Leesburg Pike, Vienna, VA 22180

C. M. WALMSLEY and T. L. WILSON: Max-Planck-Institut für Radioastronomie, Auf dem Hügel 69, 5300 Bonn 1, Federal Republic of Germany